nonchelate complex with the $[Fe_2O]^{4+}$ core thus far isolated and as such may serve as a precursor to synthetic analogues of met- and oxyhemerythrin active sites, which contain this unit.[37] $[Fe_2OCl_6]^{2-}$ has already been employed as a spectroscopic model of the oxo bridge in hemerythrin.[12a]

(37) Stenkamp, R. E.; Sieker, L. C.; Jensen, L. H.; Sanders-Loehr, J. *Nature (London)* **1981**, *291*, 263. Elan, W. T.; Stern, E. A.; McCallum, J. D.; Sanders-Loehr, J. *J. Am. Chem. Soc.* **1982**, *104*, 6369.

Acknowledgment. This research was supported by NIH Grant GM 28856. We thank Dr. J. Sola and J. Kovacs for experimental assistance.

Registry No. $(NEt_4)_2$-**1**, 62682-81-9; $(NEt_4)_2$-**2**, 87495-23-6; $(Et_4N)[FeCl_4]$, 14240-75-6; $[Fe_2S_2(SPh)_4]^{2-}$, 55939-69-0; VS(acen), 74354-70-4; VO(acen), 19195-97-2; $NbS(S_2CNEt_2)_3$, 31388-94-0; $NbO(S_2CNEt_2)_3$, 33774-12-8; $NaSSi(CH_3)_3$, 87495-22-5; $NaNH_2$, 7782-92-5; $(Me_3Si)_2S$, 3385-94-2; $NaOSiMe_3$, 18027-10-6.

Contribution from the Institut für Anorganische Chemie, CH-3000 Bern 9, Switzerland

Pair Excitations in Vivianite, $Fe_3(PO_4)_2 \cdot 8H_2O$

HANS U. GÜDEL

Received April 12, 1983

Polarized absorption spectra of the mineral vivianite, $Fe_3(PO_4)_2 \cdot 8H_2O$, were measured in the region of spin-forbidden excitations at temperatures between 6 and 100 K. The spectral range from 18 000 to 28 000 cm^{-1} is dominated by hot bands, which show a very steep rise between 6 and 50 K. They are attributed to transitions of ferromagnetically coupled iron(II) pairs arising through an exchange intensity mechanism. It is concluded that S is a good quantum number and spin–orbit coupling plays a minor role. From the observed temperature dependencies the exchange parameter of the iron(II) pairs is estimated: $2J = 5$ cm^{-1}.

Introduction

The mineral vivianite occurs naturally in various parts of the world in the form of light green-blue transparent crystals with interesting pleochroic properties.[1,2] The laboratory synthesis of $Fe_3(PO_4)_2 \cdot 8H_2O$ is complicated by the large number of iron(II) phosphate phases and the tendency of solutions and finely powdered products to oxidize in air.[3] It has so far only been prepared in polycrystalline form. The mineral vivianite has some interesting physical and chemical properties, which have been studied by several techniques.

The crystal structure determination revealed the presence of two types of iron(II) centers:[4] On site I the coordination is *trans*-$FeO_4(H_2O)_2$, point symmetry C_{2h}; the four equatorial ligands are phosphate oxygens. Two site II iron(II) ions are joined to a dimer of the edge-sharing type. This coordination is shown schematically in Figure 1. C_2 is the point symmetry of both the single ion of site II and the composite pair of site II ions. There is abundant hydrogen bonding in the anion/water structure linking the magnetic centers to a three-dimensional network.

Magnetic susceptibility[5] and heat capacity measurements[6] showed a number of magnetic anomalies between 2 and 20 K, some of which appear to be sample dependent. A transition to long-range magnetic order at 8.8 K was established by neutron diffraction.[7] The magnetic structure is antiferromagnetic, with the spins of the two iron(II) sites forming a sublattice each and a canting angle between the sublattices of 42°. The two iron(II) spins at the site II constituting the dimer are parallel, indicating ferromagnetic intradimer coupling. This magnetic structure was confirmed by Mössbauer experiments.[7]

Table I. Positions (Centers of Band Systems) and Predominant Polarizations in the 50 K Absorption Spectrum Measured Perpendicular to the *ac* Cleavage Plane of Vivianite

position, $cm^{-1} \times 10^{-3}$	dominant polarizn $\rightarrow$ ($\vec{E}$ vector)	position, $cm^{-1} \times 10^{-3}$	dominant polarizn $\rightarrow$ ($\vec{E}$ vector)
26.5	$\parallel c$	22.0	$\perp c$
25.5	$\parallel c$, $\perp c$	20.8	$\perp c$
23.5	$\parallel c$	19.5	$\perp c$

Optical absorption spectra of vivianite have been measured at room temperature.[1,2,8,9] The dominant feature in the near-infrared region is the $^5T_{2g} \rightarrow {}^5E_g$ (O_h notation) ligand field transition. It consists of two main components separated by 3500 cm^{-1}. This large splitting was attributed both to low-symmetry crystal field components[8] and to a dynamic Jahn–Teller coupling in the excited ^5E_g state.[1] In the visible part of the spectrum there is a broad and featureless absorption centered at approximately 15 200 cm^{-1}. This transition is polarized completely parallel to the b axis of the monoclinic unit cell. It is responsible for the light blue color and the pleochroism observed in vivianite. The intensity of this absorption depends on the degree of surface oxidation, and its origin is a $Fe^{2+} \rightarrow Fe^{3+}$ intervalence electron-transfer transition in the iron(II) dimers of site II.[2] A great number of iron-containing minerals exhibit absorptions of the mixed-valence type. Between 18 000 and 28 000 cm^{-1}, i.e. most of the visible region, vivianite is quite transparent. A number of very weak ($\epsilon \sim 0.1$) and rather sharp absorption bands have been reported.[1,9] In this paper we shall report and discuss low-tem-

(1) Faye, G. H.; Manning, P. G.; Nickel, E. H. *Am. Mineral.* **1968**, *53*, 1174.
(2) Burns, R. G.; Nolet, D. A.; Parkin, K. M.; McCammon, C. A.; Schwartz, K. B. In "Mixed-Valence Compounds in Chemistry, Physics and Biology"; Brown, D., Ed.; Reidel: Holland, 1979; p 295.
(3) Giovanoli, R., private communication.
(4) Mori, H.; Ito, T. *Acta Crystallogr.* **1950**, *3*, 1.
(5) Meijer, H. C.; van den Handel, J.; Frikke, E. *Physica (Amsterdam)* **1967**, *34*, 475.
(6) Forstat, H.; Love, N. D.; McElearny, J. Phys. *Rev.* **1965**, *4A*, 1246.
(7) Forsyth, J. B.; Johnson, C. E.; Wilkinson, C. *J. Phys. C* **1970**, *3*, 1127.
(8) Townsend, M. G.; Faye, G. H. *Phys. Status Solidi* **1970**, *38*, K57.
(9) Loh, E. *J. Phys. C* **1972**, *5*, 1991.

0020-1669/83/1322-3812$01.50/0

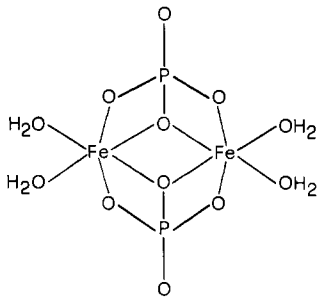

Figure 1. Coordination of the iron(II) dimer in vivianite (schematic).

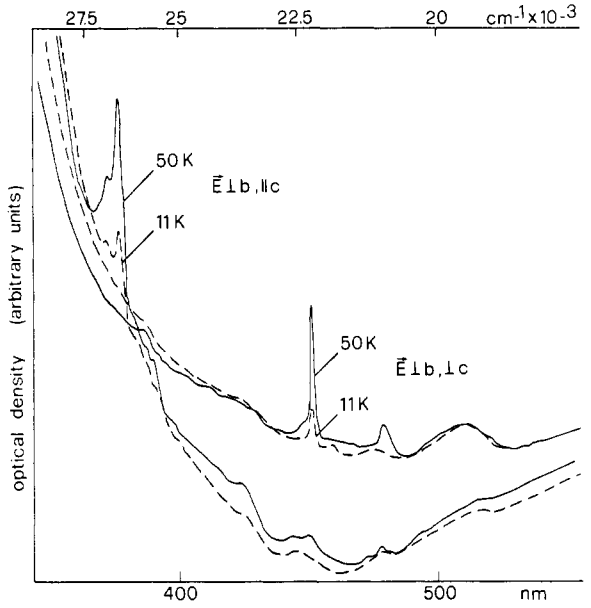

Figure 2. Polarized absorption spectrum. Light propagation is parallel to *b*.

perature measurements in this spectral range.

Experimental Section

The vivianite crystal used for this work is from Idaho and was kindly provided by R. Giovanoli. Crystal faces and unit cell directions were determined by optical and X-ray (Buerger precession camera) techniques. Polarized absorption spectra were measured on a Cary 17 spectrophotometer equipped with a matched pair of Glan–Taylor prisms. Cooling of the sample was achieved by a helium gas flow-tube technique.

Two crystal orientations were used for the absorption experiments. In the first orientation the light beam was propagating perpendicular to the naturally well-developed *ab* plane. The electric vector of the light beam could be chosen parallel and perpendicular to *b*, the two extinction directions. With $\vec{E} \parallel b$ meaningful spectra of the spin-forbidden bands could not be obtained due to the very intense intervalence electron-transfer band centered at 15 500 cm^{-1} but extending well into the visible part of the spectrum. Due to the easy cleavage parallel to the *ac* plane, thin slices could be cleaved off the bulk crystal. The extinction directions in these plates were found to lie approximately parallel and perpendicular to *c*, without any noticeable dispersion between 18 000 and 28 000 cm^{-1}. The plates were used for experiments with the light beam propagating parallel to the *b* axis.

Spectra

Figure 2 shows the polarized low-temperature absorption spectrum of a thin plate between 18 000 and 28 000 cm^{-1}. Band positions and predominant polarizations for the various band systems are listed in Table I. The most conspicuous feature of the absorption spectrum in this range is the steep drop in intensity of the band systems at 26 500, 23 500, 22 500, and 20 800 cm^{-1} when the temperature is lowered from 50 K toward liquid-helium temperature. The behavior is most pronounced for the 26 500-cm^{-1} band system, which disappears

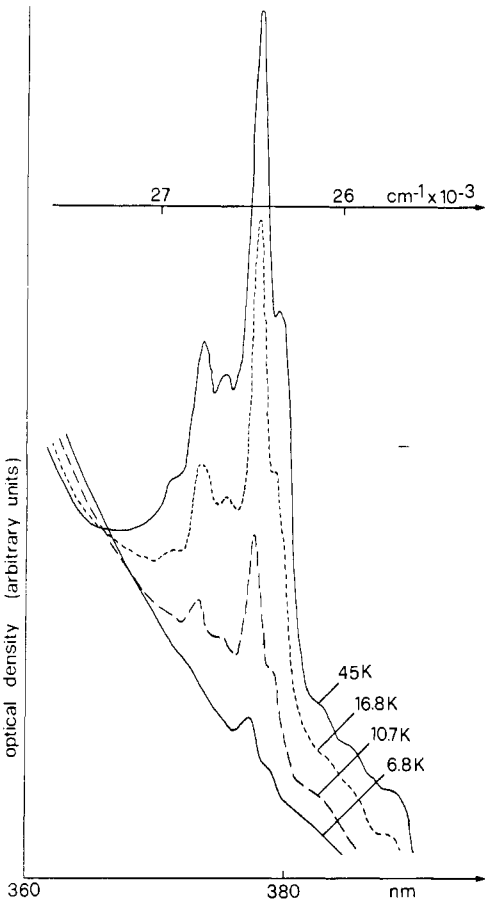

Figure 3. Temperature dependence of 26 500-cm^{-1} band system ($\vec{E} \parallel c$).

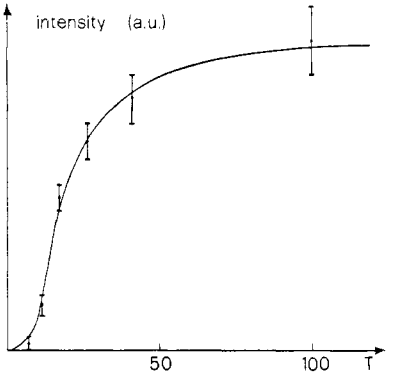

Figure 4. Integrated intensity of 26 500-cm^{-1} band system ($\vec{E} \parallel c$). The full curve is a least-squares fit of the $S = 3$ Boltzmann factor in Figure 6 to the experimental points. Parameter value: $-8J = 20$ cm^{-1}.

completely on cooling. This is shown in Figures 3 and 4. The other three bands drop essentially in the same way, but a small fraction of the intensity persists to the lowest temperatures. The 25 500-cm^{-1} band system shows intensity shifts between its components as a function of temperature (Figure 5), and the broad band centered around 19 500 cm^{-1} is practically temperature independent. The 26 500-cm^{-1} band system has no intensity with the electric vector perpendicular to *c*, the measured dichroic ratio ($\vec{E} \parallel c / \vec{E} \perp c$) being at least 40.

Discussion

There are a large number of possible spin-forbidden iron(II) excitations in the spectral range under study.[10] In addition, since the crystal is partially oxidized, there is the possibility

(10) Blazey, K. *J. Phys. Chem. Solids* **1977**, *38*, 671.

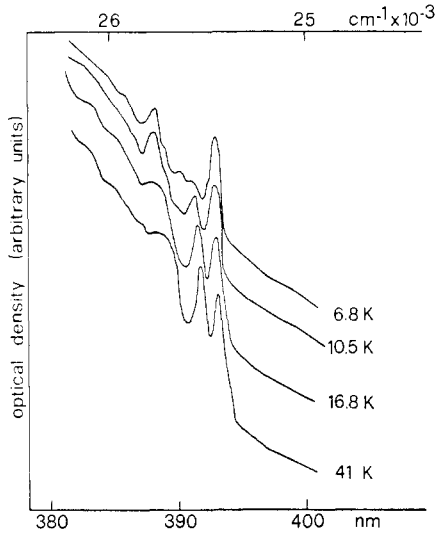

Figure 5. Temperature dependence of 25 500-cm^{-1} band system ($\vec{E} \parallel c$).

of iron(III) excitations in iron(II/III) dimers of site II, which can be strongly enhanced by an exchange intensity mechanism. Assignments of the observed absorption bands are therefore very difficult and will not be attempted here. Instead, our discussion will be focused on the striking temperature dependencies observed between 6 and 50 K.

Intensity Mechanisms. The usual intensity-gaining mechanism for spin-forbidden transitions is spin–orbit coupling in conjunction with an odd-parity crystal field component. This mechanism is a possible source of intensity in mononuclear as well as polynuclear complexes. In vivianite iron(II) site I has a center of symmetry,[4] and an odd-parity crystal field component can only be obtained through vibronic coupling. The corresponding intensity is expected to be temperature independent between 6 and 50 K and then to increase by up to 50% on increasing the temperature to 300 K. Iron site II, on the other hand, has no center of symmetry, and the intensity expected from this static odd-parity field should be more or less temperature independent.

In magnetically coupled pairs of ions there is an additional intensity mechanism for spin-forbidden excitations. It is based on the exchange interactions between the two ions.[11] The interaction with the electric vector **E** of the radiation field can be represented by

$$\mathcal{H} = \sum_{i,j} \mathbf{\Pi}_{ai,bj} \cdot \mathbf{E}(\mathbf{s}_{ai} \cdot \mathbf{s}_{bj}) \qquad (1)$$

where $\mathbf{s}_{ai}$ and $\mathbf{s}_{bj}$ are one-electron spin operators on the ions a and b. The vector components of $\mathbf{\Pi}_{ai,bj}$ are given by

$$\Pi^{\alpha}_{ai,bj} = \left(\frac{\partial J_{ai,bj}}{\partial E^{\alpha}} \right)_{E \to 0} \qquad (2)$$

$J_{ai,bj}$ is an off-diagonal exchange matrix element.

In spin-only systems this mechanism leads to the selection rule $\Delta S = 0$ for pair transitions. It has been found to be the principal source of intensity for spin-forbidden transitions in a number of exchange-coupled pairs.[12] It is particularly efficient in dimers with no center of inversion.

Discussion of the Spectra. From the observed spectra, we conclude that there are at least two different intensity mechanisms at work: A more or less temperature-independent mechanism dominates the 19 500-cm^{-1} band and contributes a small portion to all but the 26 500-cm^{-1} band. Much more important, however, is the mechanism that gives rise to the steep increase in intensity between 6 and 50 K of all the bands except for the 19 500-cm^{-1} absorption. Exchange-induced intensity is expected to show this type of behavior. Our spectrum is therefore dominated by site II iron(II) dimer absorptions.

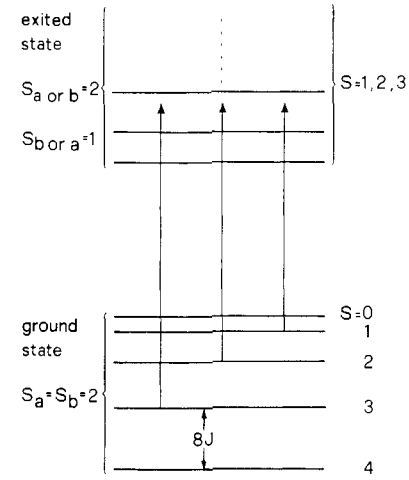

Figure 6. Schematic representation of ferromagnetic exchange splittings and $\Delta S = 0$ pair transitions.

This can be studied most clearly for the 26 500-cm^{-1} absorption band. All its intensity is hot; i.e., it drops to zero with decreasing temperature. In addition, this transition is completely polarized, with an observed dichroic ratio ($\vec{E} \parallel c / \vec{E} \perp c$) > 40. Very pure orbital selection rules must be operating. Both the intensity and polarization behavior of this transition strongly indicate that spin–orbit effects must be small in the ground and excited states. The electronic states of the iron(II) dimer are well characterized by the spin quantum number S and an orbital representation Γ. The orbital angular momentum and thus the effects of spin–orbit coupling in the $^5T_{2g}$ (O_h notation) ground state of a site II iron ion must be effectively quenched by the low-symmetry field and/or a dynamic Jahn–Teller effect. The site II iron coordination is a strongly distorted octahedron, and the low-symmetry crystal field components are therefore expected to be quite large.

We conclude that the iron site II ground state is an orbital singlet spin quintet, split by only a few wavenumbers through spin–orbit coupling. In such a situation we can try to represent the exchange coupling between the two site II iron(II) ions in the dimeric complex by a Heisenberg type Hamiltonian

$$\mathcal{H}_{ex} = -2J\mathbf{S}_a \cdot \mathbf{S}_b \qquad (3)$$

with the exchange parameter J. The corresponding splitting pattern for ferromagnetic coupling is shown in Figure 6. Electronic transitions, which are spin forbidden in a single ion, can gain intensity through the pair mechanism (eq 1). Transitions are only allowed for $\Delta S = 0$, where S is the spin quantum number of the pair states. It can take values from 0 to 4 in the pair ground state ($S_a = S_b = 2$) but only from 1 to 3 in the singly excited pair state ($S_a = 2$, $S_b = 1$). As a consequence, transitions from the lowest ground-state level, $S = 4$, are forbidden. All the intensity must be hot, in agreement with experiment. From the observed temperature dependence of intensity, we can estimate the magnitude of the exchange splitting in the ground state. Assuming the observed hot transitions to originate in the $S = 3$ ground level, we obtain an energy separation between the $S = 3$ and $S = 4$ ground levels of 20 cm^{-1} from a least-squares fit. The one-parameter fit is included in Figure 4. Its high quality gives us confidence in the simple theoretical model used. Further splittings of the pair levels resulting from spin–orbit coupling have been neglected in this estimate of exchange parameter.

(11) Ferguson, J.; Guggenheim, H. J.; Tanabe, Y. *J. Phys. Soc. Jpn.* **1966**, *21*, 692.
(12) Güdel, H. U. *Colloq. Int. CNRS* **1977**, *No. 255*, 231.

The experimentally determined energy interval of 20 cm^{-1} in the ground state could, in principle, also result from spin-orbit effects instead of exchange interactions. We exclude this possibility on the basis of the observed polarization and temperature behavior of the 26 500-cm^{-1} band. Spin-orbit coupling would relax both the spin and the orbital selection rules, which are experimentally found to be strictly followed.

The fact that vivianite orders antiferromagnetically below 8.8 K[7] has not been taken into account in our discussion. With one exception, all oure measurements were done in the paramagnetic phase, where the dominant exchange effect is the ferromagnetic coupling of the two iron(II) centers within the dimers. From the crystal structure and the observed easy cleavage perpendicular to the *b* axis, some short-range magnetic order[13] within the *ac* plane extending to temperatures above the three-dimensional-ordering temperature cannot be ruled out. However, this order, if present, is antiferromagnetic and therefore cannot be responsible for the observed hot-band behavior.[14]

The sharp rise in intensity observed for several of the spin-forbidden transitions between liquid-helium temperature and 50 K is reminiscent of the behavior of spin-forbidden bands in the quasi-two-dimensional ferromagnet $FeCl_2$.[15] The hot absorption bands in $FeCl_2$ correspond to combined exciton-magnon excitations. This means that the intensity-gaining mechanism is essentially the same as the one postulated for vivianite, namely an exchange mechanism.[14] The main difference between the two systems is the collective character of the excitations in $FeCl_2$ as a result of the extended interactions in two dimensions, whereas in vivianite the excitations are localized on the ferromagnetically coupled dimers. The ferromagnetic sign of the exchange coupling in both systems is the result of a very similar (edge-sharing) bridging geometry.

Acknowledgment. This work was financially supported by the Swiss National Science Foundation under Grant No. 2.427-0.79.

Registry No. Vivianite, 14567-67-0.

(13) Carlin, R. L.; van Duyneveldt, A. J. "Magnetic Properties of Transition Metal Compounds"; Springer-Verlag: New York, 1977; p 142.

(14) Shinagawa, K.; Tanabe, Y. *J. Phys. Soc. Jpn.* **1971**, *30*, 1280.

(15) Robbins, D. J.; Day, P. *J. Phys. C* **1976**, *9*, 867.

Contribution from the Department of Chemistry, University of Utah, Salt Lake City, Utah 84112, and the Institut für Organische Chemie, Universität Heidelberg, D-6900 Heidelberg, West Germany

Preparation, Physical Nature, and Theoretical Studies of Tetrakis(3-methylpentadienyl)trimanganese, $Mn_3(3\text{-}CH_3C_5H_6)_4$[1]

MICHAEL C. BÖHM,[2a] RICHARD D. ERNST,*[2b] ROLF GLEITER,*[2a] and DAVID R. WILSON[2b,c]

Received October 26, 1982

The synthesis and characterization of tetrakis(3-methylpentadienyl)trimanganese are reported. Detailed X-ray structural data and variable-temperature magnetic susceptibility measurements support the formulation of this material as a high-spin Mn complex (five unpaired electrons) having a nearly linear trimetallic arrangement featuring an average Mn-Mn separation of 2.516 (1) Å and ∠Mn-Mn-Mn = 177.51 (6)°. The central manganese atom also interacts with one terminal carbon atom of each 3-methylpentadienyl ligand to achieve a nearly regular *edge*-bicapped tetrahedral coordination geometry (Mn-C = 2.331 (4) Å). The structure was refined to agreement indices $R = 0.050$, $R_w = 0.072$ in space group C_i^1-$P\bar{1}$ (No. 2) with $a = 6.937$ (1) Å, $b = 7.427$ (1) Å, $c = 23.940$ (3) Å, $\alpha = 83.54$ (1)°, $\beta = 83.77$ (1)°, and $\gamma = 64.15$ (1)°. Theoretical calculations using an INDO model have been carried out for doublet, quartet, and sextet states, with the result that the quartet is much higher in energy than the doublet or sextet configurations, which possess comparable energies. The central manganese atom appears to be attached to its nearest neighbors generally by only weak covalent couplings, although strong electrostatic influences appear to be present.

Introduction

Recently it has become clear that metal-pentadienyl compounds exhibit rich and diverse chemical features. In particular, a comparison of the pentadienyl anion with the related cyclopentadienyl and allyl anions has led to expectations of both stability and chemical reactivity in the open pentadienyl-metal systems. As a result, we have been vigorously pursuing a wide range of studies in order to gain a better understanding of these systems.[3] Of initial interest have been the bis(pentadienyl)metal compounds ("open metallocenes"), which have indeed demonstrated both stability and reactivity[3] and whose orbital bonding schemes have proven quite fascinating.[4] In the course of these studies, the very unusual complex $Mn_3(3\text{-}C_6H_9)_4$ ($3\text{-}C_6H_9$ = $3\text{-}CH_3C_5H_6$) was isolated from the reaction of $MnCl_2$ with 2 equiv of the 3-methylpentadienyl anion. Preliminary data suggested that this material could best be formulated as the associated salt $Mn^{2+}[Mn(3\text{-}C_6H_9)_2^-]_2$, in which the central manganese atom very nearly possessed a regular edge-bicapped tetrahedral coordination geometry.[5] Herein we report the results of complete spectroscopic, magnetic susceptibility, X-ray diffraction, and theoretical studies designed to more precisely define the nature of the compound.

Experimental Section

All operations involving organometallics were carried out under an atmosphere of prepurified nitrogen in Schlenk apparatus or in a glovebox. Nonaqueous solvents were thoroughly dried and deoxy-

(1) (a) Electronic structure of Organometallic Compounds. 23. See ref 1b for part 22. (b) Böhm, M. C.; Gleiter, R.; Berke, H. *J. Electron Spectrosc. Relat. Phenom.*, in press.

(2) (a) Universität Heidelberg. (b) University of Utah. (c) NSF Predoctoral Fellow, 1980-present.

(3) (a) Wilson, D. R.; DiLullo, A. A.; Ernst, R. D. *J. Am. Chem. Soc.* **1980**, *102*, 5928. (b) Wilson, D. R.; Ernst, R. D.; Cymbaluk, T. H., manuscript in preparation. (c) Wilson, D. R.; Liu, J.-Z.; Ernst, R. D. *J. Am. Chem. Soc.* **1982**, *104*, 1120. (d) Liu, J.-Z.; Ernst, R. D. *Ibid.* **1982**, *104*, 3737. (e) Ernst, R. D.; Cymbaluk, T. H. *Organometallics* **1982**, *1*, 708.

(4) Böhm, M. C.; Eckert-Maksić, M.; Ernst, R. D.; Wilson, D. R.; Gleiter, R. *J. Am. Chem. Soc.* **1982**, *104*, 2699.

(5) Wilson, D. R.; Liu, J.-Z.; Ernst, R. D. *J. Am. Chem. Soc.* **1982**, *104*, 1120.

0020-1669/83/1322-3815$01.50/0